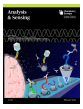

Phage-Derived and Aberrant HaloTag Peptides Immobilized on Magnetic Microbeads for Amperometric Biosensing of Serum Autoantibodies and Alzheimer's Disease Diagnosis

Alejandro Valverde[+],[a] Ana Montero-Calle[+],[b] Beatriz Arévalo,[a] Pablo San Segundo-Acosta,[b] Verónica Serafín,[a] Miren Alonso-Navarro,[b] Guillermo Solís-Fernández,[b] José M. Pingarrón,*[a] Susana Campuzano,*[a] and Rodrigo Barderas*[b]

An electrochemical biosensing platform for serum autoantibodies (AAbs) detection is reported in this work, exploiting for the first time six Alzheimer's disease (AD)-specific phage-derived and frameshift aberrant HaloTag peptides as receptors, immobilized on magnetic microbeads (MBs) surface and captured on disposable electrodes to perform amperometric detection. Operational analytical characteristics and clinical diagnostic ability of the bioplatform were probed in optimized key experimental conditions by analysing serum AAbs of AD patients and healthy subjects. The value of 100% obtained for AUC, sensitivity, and selectivity from the all peptides combined ROC curve, indicate full AD-diagnostic capability of the methodology, which was further implemented, as proof of concept, in a POC multiplexing platform to detect the signature in a single test over clinically actionable times (1 h 15 min), opening great promise for the type of diagnosis and AD patients' monitoring follow-up currently pursued.

Alzheimer's disease (AD) is the most common form of dementia in elderly age groups worldwide, with an estimated prevalence of 10–30% and an average duration of about 10 years since the first clinical symptoms.[1,2] However, AD has long preclinical and prodromal stages which extend the disease for up to 20 years.[3,4]

The diagnosis of AD through clinical data currently relies on a set of cerebrospinal fluid (CSF) and imaging biomarkers obtained by expensive and highly invasive techniques that are only available in specialized clinical settings.[5–9] Although some of them have been proven useful for AD diagnosis in the preclinical and prodromal stages, there is no strong correlation between disease progression at different preclinical stages and the levels of these biomarkers.[10,11] Thus, it is important to identify new AD-specific biomarkers using low-cost and less invasive techniques, as well as suitable biotools for their determination meeting the requirements of short assay time, simplicity, multiplexing ability, and suitability for point-of-care (POC) testing. These features will facilitate their translation to the clinic and implementation even in primary care settings to streamline and improve clinical decision making.[4]

Circulating autoantibodies (AAbs) and their target proteins have attracted great interest as promising candidate biomarkers for the early diagnosis of AD in blood.[12,13] AAbs with AD diagnostic ability have been reported against seroreactive peptides displayed on the surface of T7 phages (ANTXR1, OR8J1, PYGB and NUPR1) identified by a combination of phage display and protein microarrays, or against the peptides derived from the alternative aberrant splicing of APP and UBB (APP^{+1} and UBB^{+1}).[4,14] Phage display technology, consisting of the expression of foreign peptides or proteins outside the phage virion as a fusion with one of the phage coat proteins, has demonstrated to greatly facilitate the production of novel receptors beyond known biomolecular interactions, or against toxic or non-immunogenic targets, thus providing a valuable tool in the quest of new recognition elements for biosensor development.[15] Moreover, electrochemical biosensing has demonstrated, in connection with the use of magnetic microbeads (MBs) and HaloTag technologies, its usefulness to improve the clinical potential of specific AAbs signatures against tumor-associated antigens (TAAs) in circulation,[16,17] or from exosomes released from colorectal cancer (CRC) cell lines and tissue samples from CRC patients.[18] This methodology allowed the early and differential diagnosis of patients with premalignant lesions and CRC or other prevalent neoplasias, such as lung and breast cancers. While HaloTag technology overcome drawbacks associated with proteins that are difficult to express or purify,[19,20] MBs provide high accessible surface to be easily functionalized with a wide variety of capture ligands

[a] *A. Valverde,[+] B. Arévalo, Dr. V. Serafín, Prof. J. M. Pingarrón, Dr. S. Campuzano*
Analytical Chemistry Deparment
Faculty of Chemical Science
Complutense University of Madrid, Madrid (Spain)
E-mail: pingarro@quim.ucm.es
susanacr@quim.ucm.es
[b] *A. Montero-Calle,[+] Dr. P. San Segundo-Acosta, M. Alonso-Navarro, G. Solís-Fernández, Dr. R. Barderas*
Chronic Disease Programme, UFIEC
Institute of Health Carlos III Madrid (Spain)
E-mail: r.barderasm@isciii.es
[+] *These authors contributed equally to this manuscript*

Supporting information for this article is available on the WWW under https://doi.org/10.1002/anse.202100024

enhancing the probability of target/ligand interaction. MBs can be easily and rapidly separated from the solution which enables sensing of the target analytes in the sample solution minimizing mass transfer barriers and biofouling issues prone to occur when the sample matrix is directly exposed to the electrode surface.[21–23]

Taking advantage of our previous works using AD-specific targets of autoantibodies displayed in T7 phages or directly expressed in *E. coli* for validation as HaloTagged peptides,[4,14] we report in this work the first biosensing platform to date using this type of receptors, and the evaluation of its potential for the diagnosis of AD patients by targeting their associated AAbs. To fulfill this objective, key variables in the development of the bioplatform were optimized, its operational analytical characteristics established, and the clinical diagnostic ability evaluated by detecting AAbs against six promising AD-specific phage-derived and frameshift aberrant peptides in serum samples from AD patients and healthy individuals. In addition, as a proof of concept, the methodology was implemented in a multiplexing platform able to detect the identified AAbs signature in a single test.

Benefiting of the AD diagnostic ability of six HaloTag peptides identified by phage microarrays or as AD-specific frameshift proteins,[4,14] we have here exploited their use in the development of an electrochemical biosensing platform which enables their determination using inexpensive and handheld instrumentation, thus making it ideally suited for POC diagnostics. A detailed description of all the reagents, apparatus and protocols used for the development and application of this bioplatform is provided in the Supporting Information. The bioplatform involves the use of MBs modified with the phage-derived and frameshift aberrant HaloTag fusion peptides, previously expressed in bacteria, to efficiently and selectively capture the corresponding serum autoantibodies, and the amperometric transduction on disposable electrodes using the H_2O_2/HQ system after enzymatic labelling of the captured human IgGs with an HRP-conjugated secondary antibody (Scheme 1).

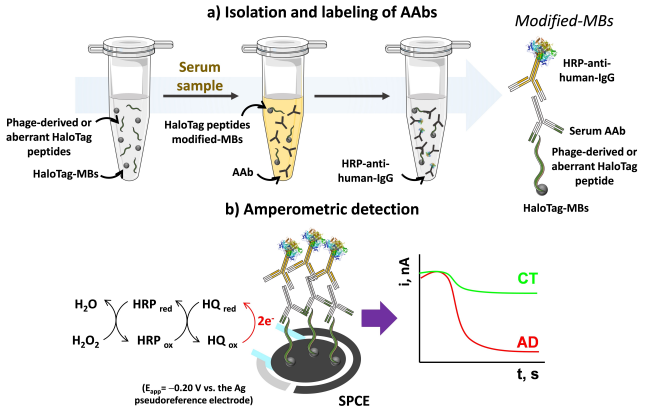

Scheme 1. Schematic diagram of the biosensing platform involving the use of MBs modified with the HaloTag peptides to efficiently capture and enzymatically label the corresponding serum AAbs (a); amperometric transduction on disposable electrodes using the H_2O_2/HQ system (b).

The amperometric responses provided by the biosensing platforms prepared using unmodified MBs and MBs modified with the 724AS control peptide and with the 94AS (NUPR1) peptide, which allowed good discrimination for sera representative of an AD patient (AD2) and a healthy individual (CT2) using luminescence immunoassays,[4] were compared. Figure S3 shows that a better discrimination (quantified by the ratio of the amperometric responses for the AD patient and the healthy individual sera, AD/CT ratio) was achieved with the bioplatforms prepared using MBs modified with the HaloTag 94AS (NUPR1) peptide.

It is worth noting that in all experiments the control peptide 724AS provided smaller responses than all the other peptides when testing AD patients' sera, whereas in control sera the responses were similar in most cases (raw data obtained for each peptide in the 20 individual serum samples after subtracting the 724AS control peptide signal are given in Table S3 in the Supporting Information).

Once the feasibility of the electroanalytical bioplatform approach was confirmed, key experimental variables were optimized. A detailed discussion of all these optimization studies is given in the Supporting Information.

The reproducibility of the measurements obtained with different bioplatforms and their storage stability was tested. Relative standard deviation (RSD) values of 3.6% and 4.0% were obtained for the amperometric responses provided by 10 different biosensing platforms prepared in the same way using HaloTag 94AS (NUPR1) peptide-MBs corresponding to serum samples of a healthy individual (CT10) and an AD patient (AD9), respectively, thus indicating the good reproducibility of the bioplatform whole construction protocol. To evaluate storage stability, the AD/CT ratio provided by bioplaftorms prepared from HaloTag 94AS (NUPR1) peptide-MBs stored since their preparation in filtered PBS buffer at 4 °C was checked. The results displayed in Figure S5 show that HaloTag 94AS (NUPR1) peptide-MBs can be stored for 12 days under the above mentioned conditions allowing the preparation of bioplatforms providing adequate discrimination in only 1 h 15 min.

The selectivity of the bioplatforms was tested by comparing the AD/CT ratio provided by the biosensing platforms prepared with HaloTag 94AS (NUPR1) peptide-MBs for 1/1,000-diluted serum samples un-supplemented or supplemented with other proteins and AAbs found in serum, such as human IgG (HIgG), hemoglobin (Hb), human serum albumin (HSA) and AAbs against dsDNA and aquaporin-4 (AQP4) at the usual expected concentrations in undiluted serum of healthy individuals.

Figure S6 shows as no significant interference was apparent in the presence of Hb, dsDNA-AAbs and AQP4-AAbs. However, the presence of IgG and HSA does interfere significantly avoiding discrimination between AD patients and healthy individuals. The interference observed in the presence of human IgG can be related to the presence of circulating human antibodies reactive with animal proteins (human anti-animal antibodies, HAAA), which are typically IgGs and recognize epitopes on the Fc portion of foreign immunoglobulins.[24] Regarding HSA, it is known that, unless highly purified, it can contain IgGs with a wide range of specificities that can disturb

the assay. Indeed, HSA interference has been described for other sandwich immunoassays for concentrations above 5 mg mL^{-1}.[25] However, no apparent interference was found when this HSA concentration was tested. In fact, considering the 1/1,000 serum dilution factor, Figure S6 shows that no significant interference from HSA and HIgG was observed when their initial concentrations were diluted in the same factor.

The diagnostic potential of the bioplatforms prepared with MBs modified with the six specific phage-derived and frameshift aberrant HaloTag peptides was assessed. Figure 1a displays the dot-plots showing the analyzed individual seroreactivity for the ten AD patients' sera (AD) and the ten healthy individuals (CT, Control). Figure 1b compares the amperometric responses provided with the bioplatforms prepared using the six HaloTag peptide-MBs for pools of AD patients and control individuals. Interestingly, nonparametric Mann-Whitney U test values indicated that statistically significant discrimination occurred between AD patients and healthy individuals with the six specific phage-derived and frameshift aberrant peptides tested. Moreover, Figure 1c displays the individual amperometric responses visualized by means of the MultiExperiment Viewer (MeV). As it can be observed, significantly different amperometric responses were obtained between AD patients and healthy individuals.

In addition, single and combined ROC curves were plotted. Figure S7 shows as all individual peptides allowed an AUC equal to or larger than 90%, sensitivities between 90% and 100% and specificities between 80% and 90% to discriminate AD patients from controls. Importantly, the combination of the results provided by the individual bioplatforms prepared with each of the 6 HaloTag peptides showed an AUC of 100% and a sensitivity and specificity of 100% for differentiating AD patients from healthy individuals.

Importantly, when the ROC curves performance was compared with those previously reported for the same phage-derived and frameshift aberrant peptides in a luminescence-based methodology (Table 1), it can be noted that the developed bioplatforms allow significant improvements in all the performance parameters. This improvement can be attributed to the extensive optimizations made in the development of these highly sensitive bioplatforms, allowing that the analyzed sera is 10-fold more diluted than that used in previous works[4,14] and providing much better sensitivity and fewer false positives.

Table S5 shows that only AD patients exhibit seroreactivity to five or six phage-derived and frameshift aberrant HaloTag peptides above the cut-off defined by the ROC curves, in contrast to healthy controls where 6 control individuals (CT2, CT3, CT5, CT6, CT9 and CT10) did not show seroreactivity to any of the peptides and only CT4 and CT7 control individuals were able to recognize up to three peptides.

The high diagnostic ability provided by the developed electroanalytical bioplatforms for discrimination of AD patients by combining the amperometric signals obtained with the individual bioplatforms for each of the six phage-derived and frameshift aberrant HaloTag peptides led us to exploit the advantages of multiplexed electrochemical detection. As a proof-of-concept, the methodology was implemented into an 8-electrode SPCE array (SP_8CE). Single batches of unmodified MBs and of MBs modified with the 724AS control peptide and the 6 specific peptides were captured on each of the working electrodes (WEs_{1-8}) of the SP_8CE and used for the sera analysis of a representative healthy subject and an AD patient. This strategy makes it possible to evaluate in a single assay the humoral response of individuals to the six specific peptides while also controlling the response obtained without peptide and with the control peptide. Figure 2a shows the amperometric responses obtained with two SP_8CE, and Figure 2b shows the actual recorded amperograms. As expected, the AD/CT

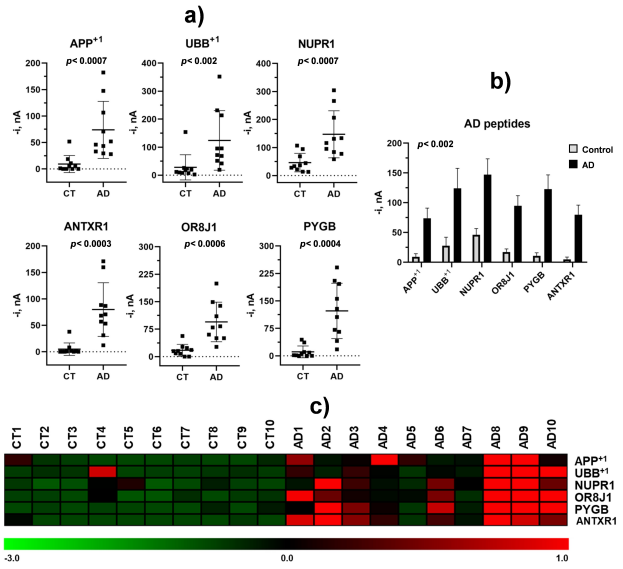

Figure 1. (a) Dot-plots displaying the analyzed seroreactivity with the bioplatforms prepared using MBs modified with each HaloTag peptide for sera of 10 individual AD patients (AD) and 10 healthy individuals (CT, Control); (b) comparison of the amperometric signals provided with the bioplatforms prepared using the six batches of HaloTag peptide-MBs with sera pools of AD patients and control individuals; non-parametric Mann-Withney U-test (*p*-value) is shown in each case. In a) and b) amperometric measurements obtained after subtracting the one recorded for the 724AS control peptide. (c) MeV visualizing of the seroreactive response of each serum for each fusion protein showing the discrimination between AD patients and controls. Green, absence or low amperometric responses; black, intermediate responses and red, large amperometric responses.

Table 1. Comparison of ROC Curve Data for single and combined phage-derived and frameshift aberrant peptides for the detection of AD Patients using the developed bioplatforms and those reported previously using a MBs-based luminescence method.[4,14]

Peptide	AUC [%][a]	Sensitivity [%][a]	Specificity, [%][a]
94AS (NUPR1)	92.0/68.9	90.0/70.6	80.0/59.6
4K16 (PYGB)	97.0/67.0	100.0/48.5	80.0/80.8
4N8 (ANTXR1)	98.0/62.0	100.0/41.2	90.0/88.5
44AM (OR8J1)	96.0/62.3	100.0/48.5	80.0/76.9
APP^{+1}	95.0/65.9	100.0/51.9	90.0/79.1
UBB^{+1}	90.0/62.0	90.0/49.4	90.0/76.0
All peptides	100.0//73.5	100.0/66.3	100.0/70.0

[a]Data achieved with the developed bioplatforms/Data reported in previous papers.[4,14]

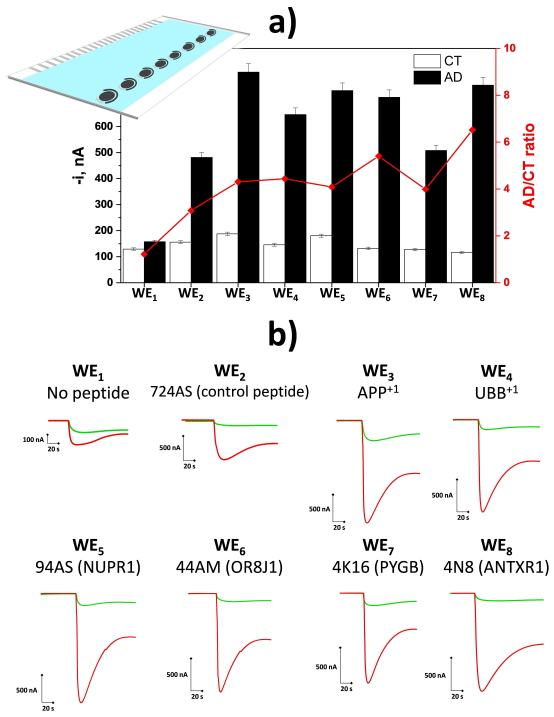

Figure 2. Comparison of the amperometric responses (a) and real amperograms (b) recorded for 1,000-diluted sera from a representative healthy individual (white bar, green line, CT) and an AD patient (black bar, red line, AD) and the corresponding AD/CT ratio (in red) using unmodified- (WE_1), control peptide- (WE_2) and the six specific peptides-modified MBs ($WEs_{3\text{-}8}$) at SP_8CEs.

ratios were consistent with those obtained individually, thus confirming the feasibility of the multiplexed methodology and the absence of cross-reactivity between adjacent electrodes. It is important to remark that although the 8-electrodes SPCE arrays are particularly suitable for this work because of the 6 specific AAbs signature identified, the developed methodology can be easily integrated into the marketed electrochemical 96× ELISA plates if more target biomarkers need to be checked.

These results confirm the possibility of a reliable and minimally invasive diagnosis of AD by analyzing AAbs against their phage-derived (ANTXR1, NUPR1, PYGB, and OR8J1), and frameshift aberrant (APP^{+1} and UBB^{+1}) HaloTagged target peptides. Importantly, the use of these novel bioreceptors *in vitro* expressed instead of purified proteins in the developed bioplatform significantly reduces cost and concerns regarding protein stability and integrity during storage. Moreover, the rationale can be used for the detection of other target biomarkers even if there are no bioreceptors available on the market and minimizes the feared batch-to-batch variations in commercially purchased reagents. These interesting features significantly improve the robustness and reproducibility required in clinical practice. In addition, the unique opportunities provided by electrochemical transduction in terms of sensitivity, simplicity, affordability, versatility, multiplexing ability, and applicability at the POC make these bioplatforms ideally suited for the type of diagnosis and AD patients' monitoring follow-up currently pursued, in contrast to CT and MRI, which require longer time and highly specialized and trained people. Despite the limited patient cohort, the capabilities and advantages demonstrated in this work reveal the potential of the developed bioplatforms to contribute to an early and reliable AD diagnosis even in outpatient settings. These differential capabilities are expected to accelerate the translation to the clinic of these biodevices with potential to improve the prognosis, life expectancy and quality of life of patients, reduce their hospital admission, the cost associated with their treatment by the Health Systems and alleviate the emotional burden of families.

Acknowledgements

The financial support of RTI2018-096135-B–I00 (Spanish Ministerio de Ciencia, Innovación y Universidades) and PID2019-103899RB–I00 (Spanish Ministerio de Ciencia e Innovación), Research Projects, PI17CIII/00045 and PI20CIII/00019 grants from the AES-ISCIII program and the TRANSNANOAVANSENS-CM Program from the Comunidad de Madrid (Grant S2018/NMT-4349) are gratefully acknowledged. A. Montero-Calle and P. San Segundo-Acosta acknowledge the support of the FPU predoctoral contracts by the Spanish Ministerio de Educación, Cultura y Deporte. A. Valverde acknowledges a predoctoral contract from Complutense University of Madrid. B. Arévalo acknowledges a predoctoral contract from the Spanish Ministerio de Economía y Competitividad (PRE2019-087596). G.S-F. is a recipient of a predoctoral contract (grant number 1193818N) supported by The Flanders Research Foundation (FWO).

Conflict of Interest

The authors declare no conflict of interest.

Keywords: Alzheimer's disease · autoantibodies · electrochemical biosensors · phage-derived peptides · receptors

[1] Y. Huang, L. Mucke, *Cell* **2012**, *148*, 1204–1222.
[2] C. L. Masters, R. Bateman, K. Blennow, C. C. Rowe, R. A. Sperling, J. L. Cummings, *Nat. Rev. Dis. Primers* **2015**, *1*, 15056. https://doi.org/10.1038/nrdp.2015.56.
[3] C. R. Jack, D. M. Holtzman, *Neuron* **2013**, *80*, 1347–1358.
[4] P. San Segundo-Acosta, A. Montero-Calle, M. Fuentes, A. Rábano, M. Villalba, R. Barderas, *J. Proteome Res.* **2019**, *18*, 2940-2953.
[5] K. Blennow, H. Hampel, M. Weiner, H. Zetterberg, *Nat. Rev. Neurol.* **2010**, *6*, 131–144.
[6] K. A. Johnson, N. C. Fox, R. A. Sperling, W. E. Klunk, Brain imaging in Alzheimer disease. *Cold Spring Harbor Perspect. Med.* **2012**, *2*, a006213. https://doi.org/10.1101/cshperspect.a006213.
[7] K. Blennow, H. Zetterberg, A. M. Fagan, *Cold Spring Harbor Perspect. Med.* **2012**, *2*, a006221. https://doi.org/10.1101/cshperspect.a006221.
[8] B. Olsson, R. Lautner, U. Andreasson, A. Ohrfelt, E. Portelius, M. Bjerke, M. Holtta, C. Rosen, C. Olsson, G. Strobel, E. Wu, K. Dakin, M. Petzold, K. Blennow, H. Zetterberg, *Lancet Neurol.* **2016**, *15*, 673–684.
[9] C. R. Jack, H. J. Wiste, S. D. Weigand, T. M. Therneau, V. J. Lowe, D. S. Knopman, J. L. Gunter, M. L. Senjem, D. T. Jones, K. Kantarci, M. M.

Machulda, M. M. Mielke, R. O. Roberts, P. Vemuri, D. A. Reyes, R. C. Petersen, *Alzheimer's Dementia* **2017**, *13*, 205–216.
[10] C. R. Jack, D. S. Knopman, W. J. Jagust, L. M. Shaw, P. S. Aisen, M. W. Weiner, R. C. Petersen, J. Q. Trojanowski, *Lancet Neurol.* **2010**, *9*, 119–128.
[11] S. Craft, A. M. Fagan, T. Iwatsubo, C. R. Jack, J. Kaye, T. J. Montine, D. C. Park, E. M. Reiman, C. C. Rowe, E. Siemers, Y. Stern, K. Yaffe, M. C. Carrillo, B. Thies, M. Morrison-Bogorad, M. V. Wagster, C. H. Phelps, *Alzheimer's Dementia* **2011**, *7*, 280–292.
[12] P. Zaenker, M. R. Ziman, *Cancer Epidemiol. Biomarkers Prev.* **2013**, *22*, 2161–2181.
[13] C. DeMarshall, A. Sarkar, E. P. Nagele, E. Goldwaser, G. Godsey, N. K. Acharya, R. G. Nagele, *Int. Rev. Neurobiol.* **2015**, *122*, 1–51.
[14] A. Montero-Calle, P. San Segundo-Acosta, Garranzo-M. Asensio, A. Rábano, R. Barderas, *Mol. Neurobiol.* **2020**, *57*, 1009–1020.
[15] R. Peltomaa, E. Benito-Peña, R. Barderas, M. C. Moreno-Bondi, *ACS Omega* **2019**, *4*, 11569–11580.
[16] M. Garranzo-Asensio, A. Guzmán-Aranguez, C. Povés, M. J. Fernández-Aceñero, R. M. Torrente-Rodríguez, V. Ruiz-Valdepeñas Montiel, G. Domínguez, L. San Frutos, N. Rodríguez, M. Villalba, J. M. Pingarrón, S. Campuzano, R. Barderas, *Anal. Chem.* **2016**, *88*, 12339–12345.
[17] M. Garranzo-Asensio, A. Guzmán-Aránguez, E. Povedano, V. Ruiz-Valdepeñas Montiel, C. Poves, M. J. Fernández-Aceñero, A. Montero-Calle, G. Solís-Fernández, S. Fernández-Diez, J. Camps, M. Arenas, E. Rodríguez-Tomàs, J. Joven, M. Sánchez-Martínez, N. Rodriguez, G. Domínguez, P. Yáñez-Sedeño, J. M. Pingarrón, S. Campuzano, R. Barderas, *Theranostics* **2020**, *10*, 3022-3034.
[18] A. Montero-Calle, I. Aranguren-Abeigon, M. Garranzo-Asensio, C. Poves, M. J. Fernández-Aceñero, J. Martínez-Useros, R. Sanz, J. Dziaková, J. Rodríguez-Cobos, G. Solís-Fernández, E. Povedano, M. Gamella, R. M. Torrente-Rodríguez, M. Alonso-Navarro, V. De los Ríos, J. I. Casal, G. Domínguez-Muñoz, A. Guzmán-Aránguez, A. Peláez-García, J. M. Pingarrón, S. Campuzano, R. Barderas. *Engineering*, in press.
[19] A. Razzaq, K. Batool, M. Aslam, A. Bhatti, *Mol. Biol.* **2021**, *10*, 1–7.
[20] R. F. Ohana, R. Hurst, J. Vidugiriene, M. R. Slater, K. V. Wood, M. Urh, *Protein Expression Purif.* **2011**, *76*, 154–164.
[21] M. E. Cortina, L. J. Melli, M. Roberti, M. Mass, G. Longinotti, S. Tropea, P. Lloret, D. A. Rey Serantes, F. Salomón, M. Lloret, A. J. Caillava, S. Restuccia, J. Altcheh, C. A. Buscaglia, L. Malatto, J. E. Ugalde, L. Fraigi, C. Moina, G. Ybarra, A. E. Ciocchini, D. J. Comerci, *Biosens. Bioelectron.* **2016**, *80*, 24–33.
[22] J. Kudr, B. Klejdus, V. Adam, O. Zitka, *TrAC Trends Anal. Chem.* **2018**, *98*, 104–113.
[23] M. Pastucha, Z. Farka, K. Lacina, Z. Mikůsova, P. Skladal, Magnetic nanoparticles for smart electrochemical immunoassays: A review on recent developments. *Microchim. Acta* **2019**, *186*, 312. https://doi.org/10.1007/s00604-019-3410-0.
[24] J. F. Emerson, K. K. Y. Lai, *Lab. Med.* **2013**, *44*, 69–73.
[25] R.-N. Zhao, Z. Feng, Y.-N. Zhao, L.-P. Jia, R.-N. Ma, W. Zhang, L. Shang, X. Qing-Wang, X. H.-S. Wang, *Talanta* **2019**, *200*, 503–510.

Manuscript received: June 29, 2021
Revised manuscript received: July 9, 2021
Accepted manuscript online: July 12, 2021
Version of record online: July 27, 2021